

Revisiting vestigial order in nematic superconductors: gauge-field mechanisms and model constraints

I. Maccari,^{1,*} E. Babaev,^{2,3} and J. Carlström^{2,4}

¹*Institute for Theoretical Physics, ETH Zurich, CH-8093 Zurich, Switzerland*

²*Department of Physics, The Royal Institute of Technology, Stockholm SE-10691, Sweden*

³*Wallenberg Initiative Materials Science for Sustainability, Department of Physics, KTH Royal Institute of Technology, SE-106 91 Stockholm, Sweden*

⁴*Department of Physics, Stockholm University, Stockholm SE-10691, Sweden*

(Dated: May 20, 2025)

The possibility that nematicity induced by electron pairing could persist above the superconducting transition temperature represents a form of composite order, sometimes referred to as a vestigial nematic phase. However, it remains debated whether—and under what conditions—such a phase can emerge in realistic models of nematic superconductors. Recent analytical work [1] concluded that vestigial nematic phases and related mechanisms do not arise in commonly used models proposed, for example, for Bi₂Se₃-based candidates. To address this question, we perform large-scale Monte Carlo simulations of a three-dimensional Ginzburg-Landau model of a nematic superconductor. Consistent with the findings of Ref. [1], our numerical results confirm that the commonly considered models do not exhibit vestigial nematic phases or nematic-fluctuation-induced charge-4e superconductivity. In the second part of the study, we investigate a different class of models and show that, under restrictive conditions, vestigial nematic order can be stabilized by an alternative mechanism: intercomponent coupling mediated by a gauge field or the effects of strong correlations.

INTRODUCTION

Significant experimental and theoretical efforts are currently directed toward identifying states characterized by order parameters composed of four fermionic fields, understanding the conditions under which such states emerge, and identifying possible candidate materials. These composite orders can emerge in systems with a superconducting ground state, resulting in an order parameter formed by four—rather than two—electrons. Although standard Bardeen-Cooper-Schrieffer (BCS) theory does not allow their formation, it has been demonstrated that these states can arise when two of the fundamental assumptions of BCS theory are violated: (i) the superconducting order parameter breaks multiple symmetries, and (ii) strong fluctuations invalidate the BCS mean-field approximation, giving rise to a regime of incoherent Cooper pairs, which still preserve broken composite symmetries[2–4].

Early theoretical examples of composite phases were considered in the $U(1) \times U(1)$ descriptions of two-dimensional superconductors. In these models, such phases emerge following a $U(1) \times U(1) \rightarrow U(1)$ transition, where the remaining broken symmetry corresponds to a four-electron composite order. This phase transition can, for example, be driven by a gauge-field-mediated intercomponent coupling [2, 3], or by the partial melting of a pair-density-wave superconducting order [5, 6]. In recent literature, these phases are often referred to as *vestigial order*. Other terms that has emerged in related contexts is *electron quadrupling condensates*, especially when referring to charge-4e, counterflow condensates, and *symmetric mass generation* [7]. In what follows, we use the term *composite order*—used in earlier studies—synonymously with vestigial order and electron quadrupling condensates,

following the usage adopted in some recent literature.

Composite orders have been studied in detail in conjunction with $U(1) \times Z_2 \rightarrow Z_2$ phase transitions. These works rely on large-scale Monte Carlo simulations of two- and three-dimensional London and Ginzburg-Landau models, covering $s+is$, $s+id$, $d+id$, and $p+ip$ and other similar states [8–10].

In general, demonstrating such states in three-dimensional models has proven to be challenging. Notably, recent works [1, 11] have shown that simple analytical methods can yield false positives across a wide range of models. Conversely, Monte Carlo simulations have demonstrated their occurrence in certain more complex systems, driven by intercomponent gauge-field coupling and/or strong correlation effects, across various symmetry-breaking scenarios:

- $U(1) \times U(1) \rightarrow U(1)$ [3, 12, 13],
- $U(1) \times Z_2 \rightarrow Z_2$ [14–16],
- $SU(2) \rightarrow O(3)$ [17–19]
- $SU(N) \rightarrow SU_n(N)$ [20].

Here, the remaining broken symmetries $U(1)$, Z_2 , $O(3)$ are associated with a four-electron composite order.

Analogous bosonic counterparts in $U(1) \times U(1) \rightarrow U(1)$ and higher symmetries, stabilized by strong interaction effects, have also been proposed and demonstrated via Monte Carlo simulations at the level of both effective field theories and fully microscopic quantum models [21–27]. The demonstration of similar composite orders was also established in high-energy physics models with various symmetries using large-scale numerical studies [28–31].

Experimentally, the most extensively studied example of the four-fermion composite order in superconducting systems is the case of a $U(1) \times Z_2 \rightarrow Z_2$

phase transition. This scenario has been investigated in $\text{Ba}_x\text{Fe}_{1-x}\text{Fe}_2\text{As}_2$ [15, 32–34], which, at low temperatures, realizes a $U(1) \times Z_2$ superconducting state that breaks time-reversal symmetry. Above the superconducting transition, the system retains long-range order associated with the phase difference between pairs of preformed Cooper pairs in different bands, thereby realizing a Z_2 electron quadrupling condensate with a rich array of novel properties [15, 32–34]. The realization of a related bosonic system with ultra-cold atoms in an optical lattice was recently reported in [35].

This work focuses on a related class of systems with multiple broken symmetries: nematic superconductors that break a $U(1) \times Z_3$ symmetry. Here, Z_3 is associated with the space-rotational symmetry. For derivations of the corresponding mean-field models, see [36–38]. Popular candidate materials for nematic superconductivity are Bi_2Se_3 -based materials [39–47]. An experimental study [48] claimed signatures of nematicity that persist above the superconducting transition temperature. The observations were interpreted in that work as evidence for a Z_3 vestigial nematic phase—i.e., rotational symmetry breaking driven by non-condensed electron pairs—within the theoretical framework proposed in Ref. [49]. Although the authors of [48] made a careful reservation that their sample does not, strictly speaking, possess Z_3 symmetry—since only one of the Z_3 states is realized upon repeated cooldowns—the study sparked new interest in the theoretical underpinnings of $U(1) \times Z_3$ superconductors. Ref. [1] presented an in-depth analytical analysis of the nematic models studied in Refs. [49, 50], and argued that these models do not support nematic vestigial phases. While this work represents the most analytically advanced treatment of the problem to date, it highlights two important directions for further investigation: (i) large-scale Monte Carlo simulations of the proposed model, and (ii) exploration of whether the composite nematic order in superconductors can occur via alternative mechanisms involving Cooper pairing.

In this work, we report large-scale Monte Carlo simulations of a three-dimensional model with a nematic superconducting ground state. Our results show that, consistent with the conclusions of [1], the basic models under consideration do not exhibit nematic order above the superconducting critical temperature. In the second part of the study, we extend the model and investigate an alternative mechanism in which composite order (vestigial nematicity) arises from intra-component coupling mediated by the gauge field. We demonstrate that this mechanism can indeed give rise to the composite nematic phase. However, it requires a very strong gauge coupling in three dimensions for this phase to be resolved, and the phase does not form generically.

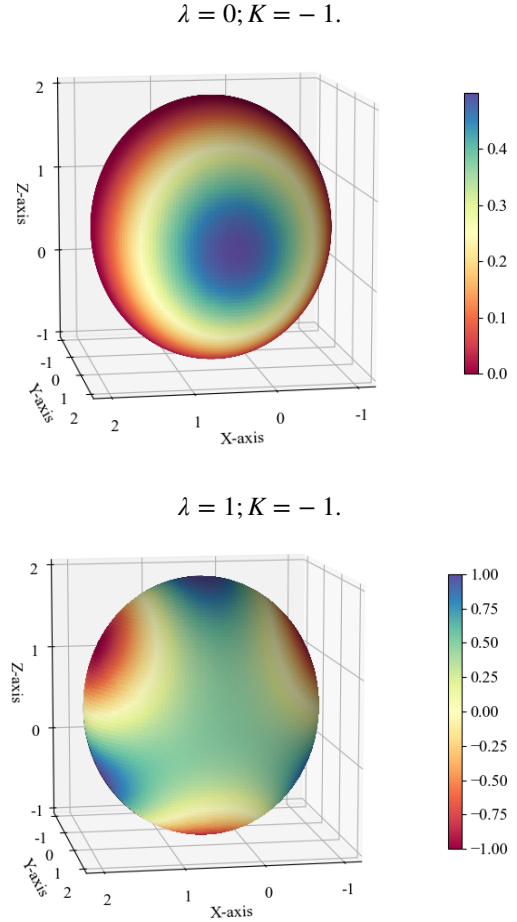


Figure 1: Nematic potential V_{nem} in Eq.(4), plotted around the unitary sphere defined by the azimuthal angle, ϕ_{12} , and the polar angle, γ . Upper panel: For $K < 0$ and $\lambda = 0$, the system has an accidental degeneracy along γ . Lower panel: The degeneracy is lifted by higher-order potential terms. For $\lambda > 0$ the potential define three equivalent minima.

THEORETICAL MODEL

We start with the simplest $U(1) \times Z_3$ Ginzburg-Landau model, which describes a two-component nematic superconducting order parameter $\vec{\Delta} = (\Delta_1, \Delta_2)$, with $\Delta_{1,2} = |\Delta_{1,2}|e^{i\phi_{1,2}}$:

$$f = \frac{1}{2} (\vec{\nabla} \times \vec{A})^2 + \frac{1}{2} \sum_{\alpha=1,2} |(\vec{\nabla} + e\vec{A}) \Delta_{\alpha}|^2 + V_{nem}(\Delta_1, \Delta_2), \quad (1)$$

where we only include the simplest gradient terms, leaving out more general contributions [1, 38, 51]. The leading potential terms, $V_{nem}(\Delta_1, \Delta_2)$, read [51, 52]

$$V(\Delta_1, \Delta_2) = \alpha_1 (|\Delta_1|^2 + |\Delta_2|^2) + \beta_1 (|\Delta_1|^2 + |\Delta_2|^2)^2 + \beta_2 |\Delta_1^2 + \Delta_2^2|^2 + \frac{\lambda}{2} [(\Delta_1 - i\Delta_2)^3 (\Delta_1^* - i\Delta_2^*)^3 + c.c.]. \quad (2)$$

In Eq. (2), the coefficient $\alpha_1 \propto (T - T_{c0})$, where T_{c0} is the characteristic temperature at which the quadratic terms change sign. Stability requires $\beta_1 > 0$ and $\beta_1 + \beta_2 > 0$, while the sign of β_2 determines the symmetry of the superconducting order parameter. The latter becomes evident when expressing the wavefunction on complex polar form, $\Delta_\alpha = |\Delta_\alpha|e^{i\phi_\alpha}$, so that

$$\beta_2 |\Delta_1^2 + \Delta_2^2|^2 = 2\beta_2 |\Delta_1|^2 |\Delta_2|^2 [\cos(2\phi_1 - 2\phi_2) - 1]. \quad (3)$$

In what follows, we will assume a fixed total density $|\Delta_1|^2 + |\Delta_2|^2 = 1$, while retaining both relative density and phase fluctuations. For convenience, we define $K = 2\beta_2$. In this scenario, the potential nematic term can be written as

$$V_{nem}(\Delta_1, \Delta_2) = -\frac{K}{2} \sum_i \sin^2(\gamma) \sin^2(\phi_{12}) + \lambda \sum_i [\cos(3\gamma) + 3\cos(\gamma) \sin^2(\gamma) \sin^2(\phi_{12})], \quad (4)$$

where $|\Delta_1| = |\cos(\gamma/2)|$, $|\Delta_2| = |\sin(\gamma/2)|$, and $\phi_{12} = \phi_1 - \phi_2$, implying $\gamma = \arctan \frac{|\Delta_2|}{|\Delta_1|}$. For $K > 0$ and $\lambda = 0$, the model describes a chiral superconducting ground state, where the intercomponent phase differences that minimize the free energy are $\phi_1 - \phi_2 = \pm\pi/2$. For $K < 0$ and $\lambda = 0$, the system has a continuous accidental degeneracy which is lifted as higher-order terms, with coupling constant λ , are included, see Fig.1.

The model Eq.(1), with $K < 0$ and $\lambda \neq 0$, exhibits, along with the superconducting $U(1)$ gauge symmetry, a Z_3 symmetry associated with three equivalent minima. Each minimum corresponds to a different, yet energetically degenerate, nematic order. As shown in the lower panel of Fig.1, for $\lambda > 0$ the three minima are:

1. $\Delta_1 = \frac{\sqrt{3}}{2}e^{i\phi}$; $|\Delta_2| = \frac{1}{2}e^{i\phi}$;
2. $\Delta_1 = \frac{\sqrt{3}}{2}e^{i\phi+\pi}$; $|\Delta_2| = \frac{1}{2}e^{i\phi}$;
3. $\Delta_1 = 0$; $|\Delta_2| = e^{i\phi}$.

By raising the temperature from a nematic superconducting ground state, composite fermionic orders emerges if the two broken symmetries are restored at different temperatures, i.e. if $T_c^{U(1)} \leq T_c^{Z_3}$. The possible emergence of these composite orders can be understood in terms of the competing proliferation of different kinds of topological defects [4]. In nematic superconductors, the relevant topological defects include skyrmionic vortices, nematic domain walls, and fractional vortices [38, 53, 54]. A composite nematic phase, for instance, can be induced by the proliferation of single-quanta skyrmionic vortices. These defects restore the $U(1)$ gauge symmetry and make the system dissipative, without disrupting the coexisting Z_3 nematic order, leading to a scenario

where $T_c^{Z_3} > T_c^{U(1)}$. Conversely, if the Z_3 domain walls—that do not carry a topological charge associated with the $U(1)$ gauge symmetry—proliferate first as the temperature increases, a charge-4e superconducting state may emerge as a composite order, as discussed in other two-dimensional [6, 55] and three-dimensional models with $U(1) \times U(1)$ symmetries [13]. In general, the separation of the two critical temperatures can be hindered by the mutual interactions among these topological defects. For example, the proliferation of skyrmionic vortices can trigger the proliferation of fractional vortices or Z_3 domain walls, and vice versa. In early works, assumptions of independent transitions led to incorrect conclusions about fluctuations in multicomponent superfluids [56] (cf. with critical discussions in different formalisms [1, 11]).

Monte Carlo methods provide a powerful tool for determining whether the system exhibits multiple phase transitions. In this work, we investigate the phase diagram of model Eq.(1) beyond the mean-field approximation by discretizing the model on a three-dimensional lattice and performing large-scale Monte Carlo simulations.

MONTE CARLO NUMERICAL RESULTS

Discretizing the model (1) we obtain:

$$H = - \sum_{i,\mu=\hat{x},\hat{y},\hat{z}} \sum_{\alpha=1,2} |\Delta_{\alpha,i}| |\Delta_{\alpha,i+\mu}| \cos \chi_{\alpha,i}^\mu + \frac{1}{2} \sum_{\nu>\mu} (F_{\mu\nu})^2 - \frac{K}{2} \sum_i \sin^2(\gamma_i) [\sin^2(\phi_{1,i} - \phi_{2,i})] + \lambda \sum_i [\cos(3\gamma_i) + 3\cos(\gamma_i) \sin^2(\gamma_i) \sin^2(\phi_{1,i} - \phi_{2,i})], \quad (5)$$

where $\chi_{\alpha,i}^\mu = \phi_{\alpha,i+\mu} - \phi_{\alpha,i} + eA_i^\mu$ is the gauge invariant superconducting phase and $F_{\mu\nu} = A_\mu(\mathbf{r}) + A_\nu(\mathbf{r} + \mu) - A_\mu(\mathbf{r} + \nu) - A_\nu(\mathbf{r})$ is the discrete form of the vector potential curl.

Each Monte Carlo step consists of 50 local Metropolis-Hastings sweeps of all lattice fields followed by a parallel tempering swap of field configurations between neighboring temperatures. Each local sweep involves the two phase fields $\phi_1(\mathbf{r}), \phi_2(\mathbf{r}) \in [0, 2\pi)$, the two amplitude fields $|\Delta_1|, |\Delta_2|$, with the constraint $|\Delta_1(\mathbf{r})|^2 + |\Delta_2(\mathbf{r})|^2 = 1$, and the vector potential field $A_\mu(\mathbf{r})$. For most of the numerical simulations, we performed a total of 20^5 Monte Carlo steps, with a transient time of maximum 20^4 Monte Carlo steps. We use standard Bootstrap resampling methods to compute errorbars.

The observables

Initially, we consider the case $e = 0$, with no coupling to the vector potential. In this scenario, we

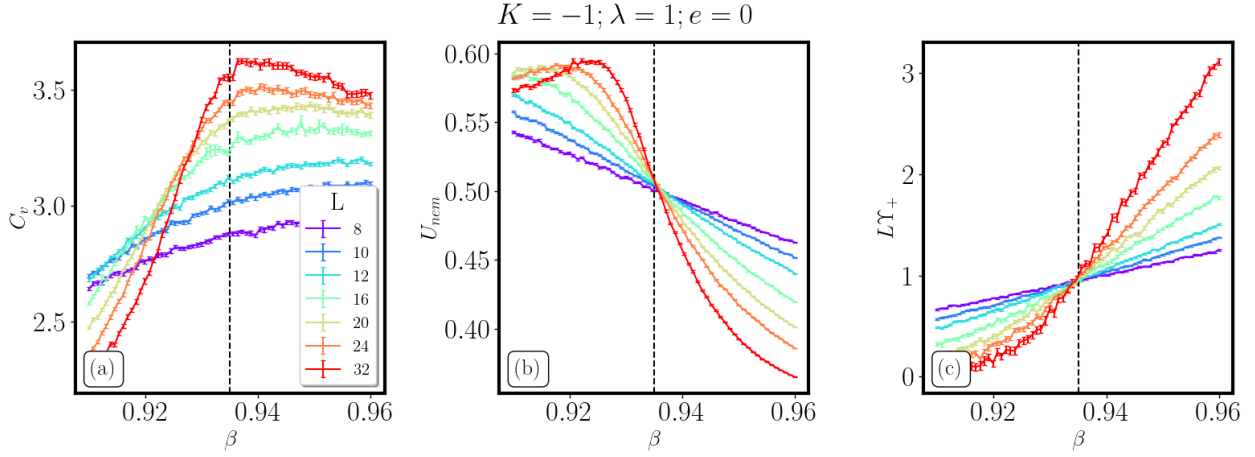


Figure 2: Monte Carlo numerical results obtained for the case $K = -1$, $\lambda = 1$ in the extreme type-II limit, i.e. $e = 0$. The three panels show (a) the specific heat, C_v , (b) the nematic Binder cumulant, U_{nem} and (c) the helicity modulus sum, Υ_+ , multiplied by the linear system size L as a function of the inverse critical temperature $\beta = 1/T$ and for different values of L . The finite-size scaling analysis reveals the presence of a single phase transition. The specific heat show a single peak and the two finite-size crossing points for U_{nem} and $L\Upsilon_+$ indicate $\beta_c^{Z_3} = \beta_c^{U(1)}$.

identify the $U(1)$ phase transition, associated with a finite superconducting order parameter, by computing the helicity modulus sum, Υ_+ , which corresponds to the superfluid stiffness. This observable is defined as the linear response to an infinitesimally small twist of the superconducting phase along a given direction $\mu = \hat{x}, \hat{y}, \hat{z}$.

$$\begin{pmatrix} \phi'_1(\mathbf{r}) \\ \phi'_2(\mathbf{r}) \end{pmatrix} = \begin{pmatrix} \phi_1(\mathbf{r}) \\ \phi_2(\mathbf{r}) \end{pmatrix} + \begin{pmatrix} \delta_\mu \cdot \mathbf{r} \\ \delta_\mu \cdot \mathbf{r} \end{pmatrix}. \quad (6)$$

The helicity modulus sum along μ is thus defined as

$$\Upsilon_+^\mu = \frac{1}{L^3} \frac{\partial^2 F(\{\phi_i\})}{\partial \delta_\mu^2} \Big|_{\delta_\mu=0} = \Upsilon_1^\mu + \Upsilon_2^\mu + 2\Upsilon_{12}^\mu, \quad (7)$$

where

$$\Upsilon_i^\mu = \frac{1}{L^3} \left[\left\langle \frac{\partial^2 H}{\partial \delta_{\mu,i}^2} \right\rangle - \beta \left\langle \left(\frac{\partial H}{\partial \delta_{\mu,i}} - \left\langle \frac{\partial H}{\partial \delta_{\mu,i}} \right\rangle \right)^2 \right\rangle \right]_{\delta=0}, \quad (8)$$

$$\Upsilon_{12}^\mu = \frac{-\beta}{L^3} \left[\left\langle \frac{\partial^2 H}{\partial \delta_{\mu,1} \partial \delta_{\mu,2}} \right\rangle - \left\langle \frac{\partial H}{\partial \delta_{\mu,1}} \right\rangle \left\langle \frac{\partial H}{\partial \delta_{\mu,2}} \right\rangle \right]_{\delta=0}. \quad (9)$$

Here, the brackets $\langle \dots \rangle$ imply thermal averages obtained via Monte Carlo simulations. For the model (5), $\Upsilon_{12}^\mu = 0$ so that $\Upsilon_+^\mu = \Upsilon_1^\mu + \Upsilon_2^\mu$. In this work, we rely on the helicity modulus sum along $\mu = \hat{x}$, and for brevity, we denote $\Upsilon_+ \equiv \Upsilon_+^x$.

When $e \neq 0$, and the gauge-field coupling is present, the onset of superconductivity is determined by measuring the Meissner effects via the so-called dual stiffness[15, 16, 18], defined as

$$\rho^\mu(\mathbf{q}) = \left\langle \frac{|\sum_{\mathbf{r}, \nu, \lambda} \epsilon_{\mu, \nu, \lambda} \Delta_\nu A_\lambda(\mathbf{r}) e^{i\mathbf{q} \cdot \mathbf{r}}|^2}{(2\pi)^2 L^3} \right\rangle. \quad (10)$$

The dual stiffness vanishes in the superconducting phase, and becomes finite in the normal state, indicating the loss of diamagnetism. Here, we compute $\rho^\mu(\mathbf{q})$ along the z -direction for a small wave vector in the x -direction, $\mathbf{q}_{min}^x = (2\pi/L, 0, 0)$, i.e. $\rho^z(\mathbf{q}_{min}^x)$, which in the following we denote simply as ρ . At the $U(1)$ critical point, similar to Υ_+^μ , the dual stiffness ρ scales as $1/L$. Thus, for $e \neq 0$, the inverse critical temperature $\beta_c^{U(1)}$ can be located from the crossing points of $L\rho$ for different linear sizes L , see Fig.4 (b).

To identify the Z_3 phase transition, associated with a finite nematic order parameter, we compute the local nematic order parameter:

$$\vec{N}_i = (N_i^x, N_i^y, N_i^z) \quad (11)$$

$$N_i^x = \Delta_{1,i} \Delta_{2,i}^* + \Delta_{1,i}^* \Delta_{2,i} \quad (12)$$

$$N_i^y = \Delta_{1,i} \Delta_{2,i}^* - \Delta_{1,i}^* \Delta_{2,i} \quad (13)$$

$$N_i^z = |\Delta_{1,i}|^2 - |\Delta_{2,i}|^2. \quad (14)$$

The nematic order parameter and the associated Binder cumulant are then defined respectively as

$$O_{Nem} = \frac{1}{L^3} [(\sum_i N_i^x)^2 + (\sum_i N_i^y)^2 + (\sum_i N_i^z)^2]^{1/2} \quad (15)$$

$$U_{nem} = \langle O_{Nem}^4 \rangle / \langle O_{Nem}^2 \rangle^2. \quad (16)$$

We identify the Z_3 critical temperature from the finite-size crossing points of U_{nem} which is expected to be universal at the critical point [57], see Fig.2(c) and Fig.4(c).

Finally, we also compute the total energy of the system and the specific heat

$$C_v = \frac{\beta^2}{L^3} (\langle H^2 \rangle - \langle H \rangle^2), \quad (17)$$

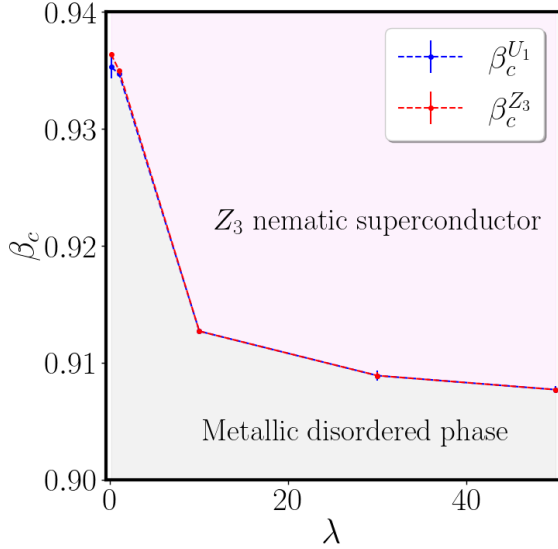


Figure 3: Phase diagram as a function of the nematic coupling λ at fixed value of $K = -1$, and in the zero gauge-field limit. The phase diagram reveals that the model at $e = 0$ does not show a vestigial phase. For all the values of λ investigated the two critical temperatures coincide. In the phase diagram, where not visible, the error bars of the data points are smaller than the marker size. For details on the extraction of critical points, see the Supplemental Material.

which is shown in Fig.2(a) and Fig.4(a).

Phase diagram in the zero gauge-field limit

We begin our investigation by considering the limit of vanishing gauge-field coupling, i.e., $e = 0$, which corresponds to a neutral system or to an extreme type II superconducting regime, characterized by a divergent London penetration depth $\lambda_L \propto 1/e \rightarrow \infty$.

In the limit $\lambda = K = 0$, the model is $SU(2)$ symmetric and shows a single phase transition in the zero gauge-field limit [17, 19, 20]. Finite values of λ reduce the symmetry of the system from $SU(2)$ to $U(1) \times Z_3$. This leads to a reduced configuration space for fluctuations associated with the phase difference mode, resulting in an increased critical temperature for the Z_3 nematic order as a function of λ . Consequently, as λ increases, the only possible separation of the two critical temperatures is such that $T_c^{Z_3} > T_c^{U(1)}$.

We consider the model in Eq.(5) for various values of λ at a fixed $K = -1$. The numerical results for the case $\lambda = 1$, $K = -1$, and $e = 0$ are summarized in Fig. 2. Finite-size scaling analysis indicates that the system undergoes a single phase transition from a nematic superconducting ground state to a disordered metallic phase. The single-transition scenario appears to hold throughout the range of λ values examined. As shown in the phase diagram in Fig. 3, the two critical

temperatures remain indistinguishable— within error bars— for all the values of λ investigated, including very large values of the coupling constant. Further details on the finite-size scaling analysis used to extract the critical points are provided in the Appendix. As evident in Fig. 3, in the limit $\lambda \rightarrow \infty$, the critical temperatures saturate due to the discrete lattice, which imposes a minimal size for the Z_3 domain walls separating different nematic configurations. Taken together, our results suggest that for $e = 0$, the model in Eq.(5) does not exhibit a resolvable separation between the two critical temperatures and thus does not support the emergence of a composite ordered phase, in accordance with the findings of Ref. [1].

Phase diagram as a function of the gauge-field coupling

We now consider the case of finite gauge field coupling, i.e. $e \neq 0$. For convenience, we rewrite the free energy density Eq.(1) as

$$f = \frac{1}{2\rho^2} \left[|\Delta_1|^2 \vec{\nabla} \phi_1 + |\Delta_2|^2 \vec{\nabla} \phi_2 + e\rho^2 \vec{A} \right]^2 + \frac{|\Delta_1|^2 |\Delta_2|^2}{2\rho^2} \left[\vec{\nabla}(\phi_1 - \phi_2) \right]^2 + \frac{1}{2} \left[(\vec{\nabla}|\Delta_1|)^2 + (\vec{\nabla}|\Delta_2|)^2 \right] + V_{nem}(\Delta_1, \Delta_2) + \frac{1}{2} (\vec{\nabla} \times \vec{A})^2, \quad (18)$$

with $\rho^2 = |\Delta_1|^2 + |\Delta_2|^2 = 1$. The electromagnetic field in Eq.(18) couples to the co-flow of the two components, and thereby reduces the energy cost of skyrmionic vortices that carry integer flux [38]. Consequently, gauge field coupling drives fluctuations in the $U(1)$ sector and will eventually lead to a separation of the phase transitions so that $T_c^{Z_3} > T_c^{U(1)}$, provided that e is sufficiently large. This will give rise to a non-superconducting composite order state that breaks the Z_3 nematic symmetry.

Our simulations confirm this scenario. For gauge couplings $e < 3.5$, within the accuracy of our calculations, the system exhibits a single phase transition from a nematic superconductor to a metallic, disordered phase. However, upon further increasing the gauge coupling, we observe a clear splitting of the two phase transitions. In Fig. 4, we show the specific heat, the nematic Binder cumulant, and the dual stiffness as functions of inverse temperature β for $e = 3.8$. Here, the two inverse critical temperatures are distinctly separated, with $\beta_c^{Z_3} < \beta_c^{U(1)}$, and the specific heat displays two well-defined peaks corresponding to the Z_3 nematic and the $U(1)$ superconducting transitions.

The phase diagram, as a function of the electric charge e , is shown in Fig. 5. As discussed in the Appendix, our numerical simulations indicate that close to the bicritical point where the two critical temper-

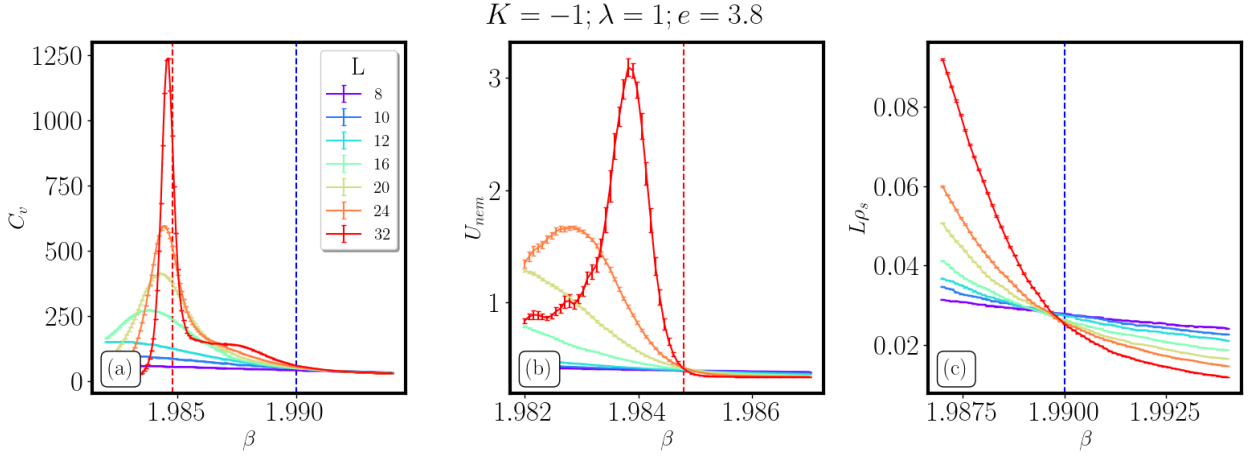


Figure 4: Monte Carlo numerical results obtained for the case $K = -1$, $\lambda = 1$ and $e = 3.8$. The three panels show (a) the specific heat, C_v , (b) the nematic Binder cumulant, U_{nem} and (c) the dual stiffness, ρ_s , multiplied by the linear system size L , as a function of the inverse critical temperature $\beta = 1/T$ and for different values of L . These numerical results reveal the presence of two distinct phase transitions. The specific heat shows two peaks associated with the Z_3 and $U(1)$ critical points, identified via the finite-size scaling analysis of U_{nem} and $L\rho_s$, respectively. For these values of the parameters $\beta_c^{Z_3} < \beta_c^{U(1)}$, which shows the emergence of a nematic nonsuperconducting state at intermediate temperatures, i.e. for $\beta_c^{Z_3} < \beta < \beta_c^{U(1)}$.

atures separate, the transition acquires a more pronounced first-order character.

Electromagnetic stabilization of the nematic composite order

Our numerical results have revealed that, in three spatial dimensions, a nematic composite order is observable only for large values of the intercomponent gauge-field coupling, i.e. $e > 3.5$. However, in two spatial dimensions, the conditions for realizing such a phase are less restrictive.

In two dimensions, the inclusion of a gauge-field coupling alters the energetics of topological defects: it renders the energy cost of creating defects that carry an integer number of flux quanta finite. In nematic systems, these defects typically take the form of skyrmionic vortices, which also possess finite energy [38, 58]. As a result, the arguments presented in Ref. [2] become directly applicable: while superconducting order is destroyed at any finite temperature due to thermal fluctuations in the thermodynamic limit, the discrete Z_3 nematic order can remain stable and persist to finite temperatures.

In three dimensions, the situation differs markedly. Unlike in two dimensions, superconductivity can survive at finite temperatures because of the finite line tension of vortices. In a three-dimensional nematic system, skyrmionic vortices have a finite energy per unit length, creating a significant energetic obstacle to their proliferation. This results in the difficulty of stabilizing a composite nematic order in simple three-dimensional nematic models without invoking additional mechanisms.

An alternative way to enlarge the parameter space to stabilize a nematic composite order is by suppressing superconductivity externally, for instance, by applying an external magnetic field, inducing a dilute su-

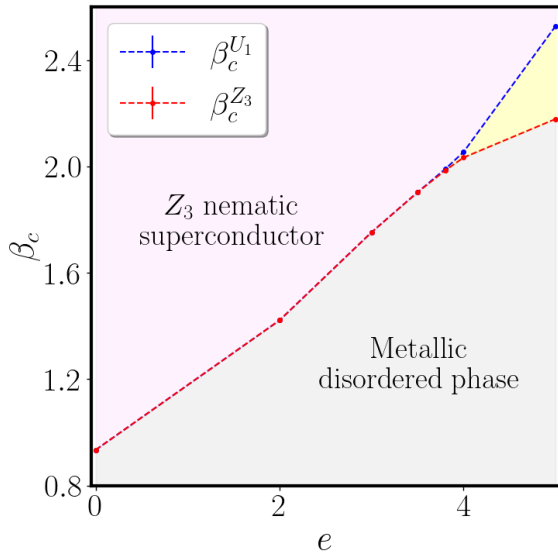


Figure 5: Phase diagram as a function of the electric charge e for the free energy with parameters $\lambda = |K| = 1$. Where not visible, the error bars of the data points are smaller than the marker size. This phase diagram reveals that a composite nematic phase can be resolved at large enough values of the electric charge $e > 3.5$.

perconducting vortex lattice. Such a vortex lattice can be melted with relatively weak thermal fluctuations, thereby restoring the gauge symmetry, while leaving the nematic symmetry broken. Thus, we propose that a composite nematic state in three-dimensional superconductors could be catalyzed through vortex lattice melting induced by an external magnetic field. In addition to the standard signatures of nematic order, one should observe a distinct specific heat anomaly in the vortex liquid phase above the latent heat peak associated with the melting transition.

CONCLUSIONS

In summary, we have conducted large-scale Monte Carlo simulations to assess the propensity for composite/vestigial order in three-dimensional nematic superconductors. In the absence of gauge-field coupling, our results show a single phase transition from a nematic superconducting state to a disordered phase, with no evidence of an intermediate composite order/vestigial state. Our simulations are consistent with analytical calculations presented in [1].

When gauge-field coupling is included, we observe that a vestigial nematic order—corresponding to a four-electron composite order with broken Z_3 symmetry—emerges above the superconducting transition. Yet, it is only resolvable in our model for very strong gauge coupling ($e > 3.5$). While this serves as a proof of principle, it also suggests that the realization of such phases via a gauge-field coupling in materials similar to Bi_2Se_3 -based candidates may require suppressing the superconducting transition by applying an external magnetic field—following an argument similar to that in Refs. [3, 12]—which leads to the melting of a dilute lattice of nematic skyrmionic vortices. Alternatively, these phases could be stabilized in the absence of an external field through additional intercomponent interactions, such as mixed gradient terms, arising, for example, from strong correlations, similar to those considered in Refs. [15, 16].

ACKNOWLEDGMENTS

The computations were enabled by resources provided by the National Academic Infrastructure for Supercomputing in Sweden (NAISS), partially funded by the Swedish Research Council through grant agreement no. 2022-06725. EB was supported by the Swedish Research Council Grants 2022-04763, by Olle Engkvists Stiftelse, and partially by the Wallenberg Initiative Materials Science for Sustainability (WISE) funded by the Knut and Alice Wallenberg Foundation. JC was supported by the Swedish Research Council (VR) through grant 2018-03882. IM acknowledges financial support by the Swiss National Science Foundation (SNSF) via the SNSF postdoctoral Grant

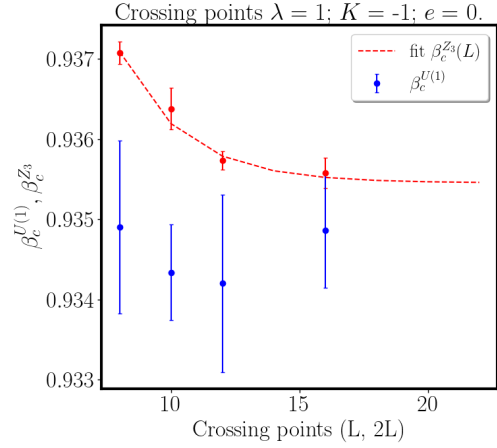


Figure 6: Finite-size scaling of the crossing points $\beta_c^{Z_3}$ and $\beta_c^{U(1)}$ extracted from the nematic Binder cumulant and the helicity modulus sum for the case $e = 0$, $\lambda = 1$, and $K = -1$.

No. TMPFP2_217204. JC and IM were supported by the Carl Trygger foundation through Grant No. CTS 20:75. JC and EB were supported by a project grant from Knut och Alice Wallenbergs Stiftelse.

APPENDIX A: ASSESSMENT OF THE CRITICAL POINTS

To assess the critical temperatures $U(1)$ and Z_3 , we extract the finite-size crossing points of the relevant observables and extrapolate their thermodynamic values. Here, we use as ansatz the finite-size scaling of their corresponding universality class.

The superconducting $U(1)$ phase transition, at $e = 0$, belongs to the same universality class as the three-dimensional XY model, whose inverse critical temperature finite-size scaling reads [59]

$$\beta_c^{U(1)}(L) = \beta_c^{U(1)}(\infty) + bL^{1/\nu}. \quad (19)$$

We used the same ansatz for case $e \neq 0$.

On the other hand, the nematic Z_3 phase transition has the same universality class as the three-state Potts model, which exhibits in three spatial dimensions a weak first-order phase transition [60, 61]. Thus, we use the corresponding finite-size scaling [61]:

$$\beta_c^{Z_3}(L) = \beta_c^{Z_3}(\infty) + be^{-\nu L}. \quad (20)$$

Let us highlight that these scaling functions do not have to necessarily hold for our model Eq.5, since in a wide range of the parameter space the system undergoes a single $U(1) \times Z_3$ phase transition, which is expected to be first order.

An example of the extrapolation of the two critical temperatures through these two scaling functions is shown in Fig.7.

For the cases where we could not properly fit the finite-size crossing points via Eqs.(19)-(20), we take

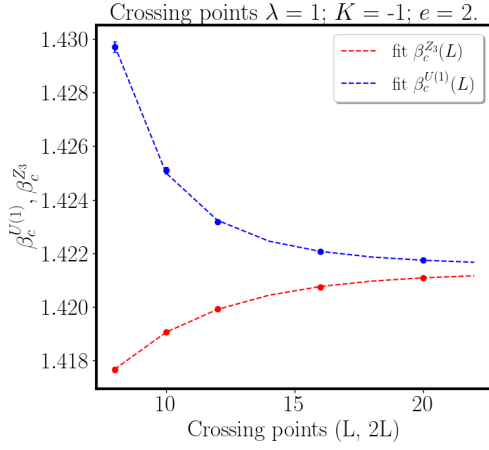


Figure 7: Finite-size scaling of the crossing points $\beta_c^{Z_3}$ and $\beta_c^{U(1)}$ extracted from the nematic Binder cumulant and the dual stiffness for the case $e = 2.0$, $\lambda = 1$, and $K = -1$. The two fitting functions give $\beta_c^{U(1)} = \beta_c^{Z_3} = 1.421$.

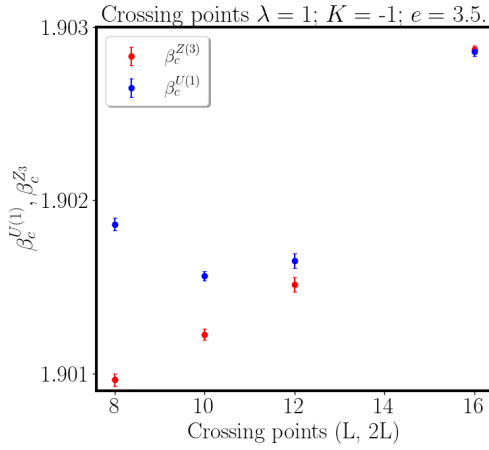


Figure 8: Finite-size scaling of the crossing points $\beta_c^{Z_3}$ and $\beta_c^{U(1)}$ extracted from the nematic Binder cumulant and the dual stiffness for the case $e = 3.5$, $\lambda = 1$, and $K = -1$. The strong drift of the crossing points is another indication of the proximity to a critical point where the two phase transitions split apart.

the crossing point of the largest finite sizes, for example, the one of $(L, 2L) = (16, 32)$ in Fig.6 and Fig.8. Finally, it is worth noticing that by increasing the value of the gauge coupling e , and approaching the point at which the two phase transitions split apart, the transition acquires a more pronounced first-order character which manifests itself in a double-peak feature of the energy distribution, see panel (c) of Fig.9. This is similar to other multicomponent models considered in other contexts [17, 23]. At the same time, by approaching the bicritical point, the finite-size effects also become much more pronounced, as is visible from the finite-size analysis of the crossing points shown in Fig.8.

* imaccari@phys.ethz.ch

- [1] P. T. How and S. K. Yip, Physical Review B **107**, 104514 (2023), publisher: American Physical Society.
- [2] E. Babaev, arXiv preprint cond-mat/0201547 (2002).
- [3] E. Babaev, A. Sudbø, and N. W. Ashcroft, Nature **431**, 666 (2004), number: 7009 Publisher: Nature Publishing Group.
- [4] B. Svistunov, E. Babaev, and N. V. Prokof'ev, *Superfluid states of matter* (CRC Press, 2015) pages: 1-546.
- [5] D. F. Agterberg and H. Tsunetsugu, Nature Physics **4**, 639 (2008), bandiera_abtest: a Cg_type: Nature Research Journals Number: 8 Primary_atype: Research Publisher: Nature Publishing Group.
- [6] L. Radzihovsky and A. Vishwanath, Physical Review Letters **103**, 010404 (2009), publisher: American Physical Society.
- [7] N. Butt, S. Catterall, and G. C. Toga, Symmetry **13**, 2276 (2021).
- [8] T. A. Bojesen, E. Babaev, and A. Sudbø, Physical Review B **88**, 220511 (2013), publisher: American Physical Society.
- [9] I. Maccari, J. Carlström, and E. Babaev, Physical Review B **107**, 064501 (2023), publisher: American Physical Society.
- [10] P. T. How and S. K. Yip, Physical Review B **110**, 054519 (2024), publisher: American Physical Society.
- [11] A. C. Yuan, Physical Review B **109**, 094509 (2024), publisher: American Physical Society.
- [12] E. Smørgrav, E. Babaev, J. Smiseth, and A. Sudbø, Physical Review Letters **95**, 135301 (2005).
- [13] E. V. Herland, E. Babaev, and A. Sudbø, Physical Review B **82**, 134511 (2010).
- [14] T. A. Bojesen, E. Babaev, and A. Sudbø, Physical Review B **89**, 104509 (2014), publisher: American Physical Society.
- [15] V. Grinenko, D. Weston, F. Caglieris, C. Wuttke, C. Hess, T. Gottschall, I. Maccari, D. Gorbunov, S. Zherlitsyn, J. Wosnitza, A. Rydh, K. Kihou, C.-H. Lee, R. Sarkar, S. Dengre, J. Garaud, A. Charnukha, R. Hühne, K. Nielsch, B. Büchner, H.-H. Klauss, and E. Babaev, Nature Physics, 1 (2021).
- [16] I. Maccari and E. Babaev, Physical Review B **105**, 214520 (2022), publisher: American Physical Society.
- [17] A. B. Kuklov, M. Matsumoto, N. V. Prokof'ev, B. V. Svistunov, and M. Troyer, Physical Review Letters **101**, 050405 (2008), publisher: American Physical Society.
- [18] O. I. Motrunich and A. Vishwanath, arXiv:0805.1494 [cond-mat] (2008), arXiv: 0805.1494.
- [19] E. V. Herland, T. A. Bojesen, E. Babaev, and A. Sudbø, Physical Review B **87**, 134503 (2013), publisher: American Physical Society.
- [20] D. Weston and E. Babaev, Physical Review B **104**, 075116 (2021), publisher: American Physical Society.
- [21] A. B. Kuklov and B. V. Svistunov, Physical Review Letters **90**, 100401 (2003), publisher: American Physical Society.
- [22] E. Altman, W. Hofstetter, E. Demler, and M. D. Lukin, New Journal of Physics **5**, 113 (2003).
- [23] A. B. Kuklov, N. V. Prokof'ev, B. V. Svistunov, and M. Troyer, Annals of Physics July 2006 Special Issue, **321**, 1602 (2006).
- [24] A. Kuklov, N. Prokof'ev, and B. Svistunov, Physical Review Letters **92**, 030403 (2004).

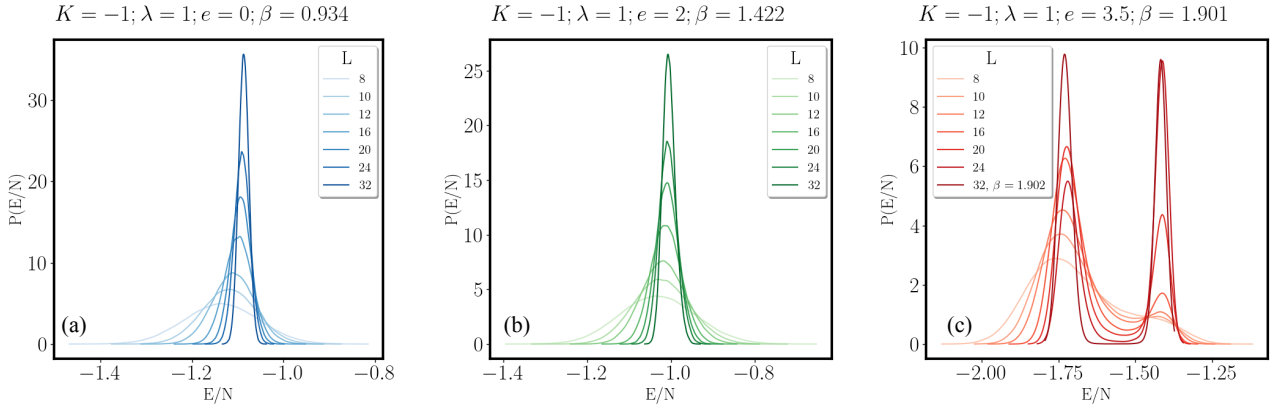


Figure 9: Probability distribution of the energy per lattice site, E/N , for different values of the linear size at the critical point and with system parameters $\lambda = 1$, $K = -1$, and: (a) $e = 0$; (b) $e = 2.0$; (c) $e = 3.5$. By increasing the value of the gauge coupling and approaching the critical value at which the two phase transitions split apart, we identify a possible tricritical point where a second order phase transition, for small values of e , turns into a first order phase transition at $e > 2$. The assessment of this tricritical point is beyond the scope of the present work.

- [25] S. G. Söyler, B. Capogrosso-Sansone, N. V. Prokof'ev, and B. V. Svistunov, *New Journal of Physics* **11**, 073036 (2009).
- [26] K. Sellin and E. Babaev, *Physical Review B* **97**, 094517 (2018), publisher: American Physical Society.
- [27] E. Blomquist, A. Syrwid, and E. Babaev, *Physical Review Letters* **127**, 255303 (2021), publisher: American Physical Society.
- [28] C. Bonati, A. Pelissetto, and E. Vicari, *Physical Review D* **109**, 034517 (2024).
- [29] C. Bonati, A. Pelissetto, and E. Vicari, *Physical Review B* **108**, 245154 (2023).
- [30] C. Bonati, A. Pelissetto, and E. Vicari, *Physical Review E* **109**, 044146 (2024).
- [31] N. Butt, S. Catterall, and A. Hasenfratz, *Physical Review Letters* **134**, 031602 (2025), publisher: American Physical Society.
- [32] I. Shipulin, N. Stegani, I. Maccari, K. Kihou, C.-H. Lee, Q. Hu, Y. Zheng, F. Yang, Y. Li, C.-M. Yim, R. Hühne, H.-H. Klauss, M. Putti, F. Caglieris, E. Babaev, and V. Grinenko, *Nature Communications* **14**, 6734 (2023), number: 1 Publisher: Nature Publishing Group.
- [33] C. Halcrow, I. Shipulin, F. Caglieris, Y. Li, K. Kihou, C.-H. Lee, H.-H. Klauss, S. Zherlitsyn, V. Grinenko, and E. Babaev, "Probing electron quadrupling order through ultrasound," (2024), arXiv:2404.03020 [cond-mat, physics:quant-ph].
- [34] F. Bärthl, N. Stegani, F. Caglieris, I. Shipulin, Y. Li, Q. Hu, Y. Zheng, C.-M. Yim, S. Luther, J. Wosnitza, *et al.*, arXiv preprint arXiv:2501.11936 (2025).
- [35] Y.-G. Zheng, A. Luo, Y.-C. Shen, M.-G. He, Z.-H. Zhu, Y. Liu, W.-Y. Zhang, H. Sun, Y. Deng, Z.-S. Yuan, and J.-W. Pan, *Nature Physics* **21**, 208 (2025), publisher: Nature Publishing Group.
- [36] L. Fu and E. Berg, *Physical Review Letters* **105**, 097001 (2010), publisher: American Physical Society.
- [37] L. Fu, *Phys. Rev. B* **90**, 100509 (2014).
- [38] A. Zyuzin, J. Garaud, and E. Babaev, *Physical Review Letters* **119**, 167001 (2017), publisher: American Physical Society.
- [39] K. Matano, M. Kriener, K. Segawa, Y. Ando, and G.-q. Zheng, *Nature Physics* **12**, 852 (2016), publisher: Nature Publishing Group.
- [40] Y. Pan, A. M. Nikitin, G. K. Araizi, Y. K. Huang, Y. Matsushita, T. Naka, and A. de Visser, *Scientific Reports* **6**, 28632 (2016).
- [41] J. W. F. Venderbos, V. Kozii, and L. Fu, *Physical Review B* **94**, 094522 (2016), publisher: American Physical Society.
- [42] T. Asaba, B. Lawson, C. Tinsman, L. Chen, P. Corbae, G. Li, Y. Qiu, Y. Hor, L. Fu, and L. Li, *Physical Review X* **7**, 011009 (2017), publisher: American Physical Society.
- [43] S. Yonezawa, K. Tajiri, S. Nakata, Y. Nagai, Z. Wang, K. Segawa, Y. Ando, and Y. Maeno, *Nature Physics* **13**, 123 (2017), publisher: Nature Publishing Group.
- [44] J. Shen, W.-Y. He, N. F. Q. Yuan, Z. Huang, C.-w. Cho, S. H. Lee, Y. S. Hor, K. T. Law, and R. Lortz, *npj Quantum Materials* **2**, 1 (2017), publisher: Nature Publishing Group.
- [45] M. P. Smylie, K. Willa, H. Claus, A. E. Koshelev, K. W. Song, W.-K. Kwok, Z. Islam, G. D. Gu, J. A. Schneeloch, R. D. Zhong, and U. Welp, *Scientific Reports* **8**, 7666 (2018), publisher: Nature Publishing Group.
- [46] S. Yonezawa, *Condensed Matter* **4**, 2 (2019), number: 1 Publisher: Multidisciplinary Digital Publishing Institute.
- [47] P. T. How and S.-K. Yip, *Physical Review B* **100**, 134508 (2019), publisher: American Physical Society.
- [48] C.-w. Cho, J. Shen, J. Lyu, O. Atanov, Q. Chen, S. H. Lee, Y. S. Hor, D. J. Gawryluk, E. Pomjakushina, M. Bartkowiak, *et al.*, *Nature communications* **11**, 3056 (2020).
- [49] M. Hecker and J. Schmalian, *npj Quantum Materials* **3**, 1 (2018), number: 1 Publisher: Nature Publishing Group.
- [50] R. M. Fernandes, P. P. Orth, and J. Schmalian, *Annual Review of Condensed Matter Physics* **10**, 133 (2019).
- [51] M. Sigrist and K. Ueda, *Reviews of Modern Physics* **63**, 239 (1991), publisher: American Physical Society.
- [52] D. V. Chichinadze, L. Classen, and A. V. Chubukov, *Physical Review B* **101**, 224513 (2020), publisher: American Physical Society.
- [53] P. T. How and S.-K. Yip, *Physical Review Research* **2**, 043192 (2020).
- [54] F. Wu and I. Martin, *Physical Review B* **95**, 224503 (2017).
- [55] E. Berg, E. Fradkin, and S. A. Kivelson, *Nature Physics* **5**, 830 (2009).
- [56] S. Korshunov, *Zh. Eksp. Teor. Fiz* **89**, 539 (1985).
- [57] K. Binder, *Physical Review Letters* **47**, 693 (1981), publisher: American Physical Society.
- [58] M. Speight, T. Winyard, and E. Babaev, *Physical Review Letters* **130**, 226002 (2023).
- [59] M. Campostrini, M. Hasenbusch, A. Pelissetto, P. Rossi, and E. Vicari, *Phys. Rev. B* **63**, 214503 (2001).
- [60] F. Y. Wu, *Reviews of Modern Physics* **54**, 235 (1982), publisher: American Physical Society.
- [61] W. Janke and R. Villanova, *Nuclear Physics B* **489**, 679 (1997).